Influence of Bases on Hydrothermal Synthesis of Titanate Nanostructures

Lucky M. Sikhwivhilu, [1] Suprakas Sinha Ray, [1,] * and Neil J. Coville[2]

[1]*National Centre for Nano-Structured Materials, Council for Scientific and Industrial Research, Pretoria 0001, Republic of South Africa.*
[2]*School of Chemistry, University of Witwatersrand, Johannesburg 2050, Republic of South Africa*

A hydrothermal treatment of titanium dioxide (TiO_2), with various bases (*i.e.* LiOH, NaOH, KOH and NH_4OH), was used to prepare materials with unique morphologies, relatively small crystallite sizes, and large specific surface areas. The experimental results show that the formation of TiO_2 is largely dependent on the type, strength and concentration of a base. The effect of the nature of the base used and the concentration of the base on the formation of nanostructures were investigated using X-ray diffraction, Raman spectroscopy, transmission and scanning electron microscopy, as well as surface area measurements. Sodium hydroxide (NaOH) and potassium hydroxide (KOH) were both used to transform the morphology of starting TiO_2 material.

*Corresponding author.
E-mail: rsuprakas@csir.co.za Fax: +27 (012) 841 2135

I. Introduction

The synthesis of one-dimensional (1-D) nanostructures, such as nanotubes, nanowires, nanobelts and nanorods, has generated great interest because of their unique structural properties, size effects and potential applications in optical and electronic devices. Titania, also known as titanium dioxide, is a widely studied material due to its photocatalytic activity, biological and chemical inertness, and its corrosion durability, especially with regard to the first two mentioned. [1-4]Although TiO_2 is a promising material for applications in photocatalytic oxidation and gas sensing technologies, the low specific surface area and photocatalytic efficiency remain barriers to overcome. This clearly indicates that further improvement of photocatalytic activity is crucial in terms of practical use and commercialization. In order to achieve this it is, therefore, desirable to enhance photocatalytic activity by synthesizing nanocrystalline TiO_2 material with small particle-size and large specific surface area. Successful attempts to synthesize mesoporous TiO_2 with large surface area and improved photocatalytic activity have been reported using conventional methods in the presence of various surfactants as templates. The setback is that the produced material requires the removal of these templates by thermal means in order to obtain the final crystalline product. [5, 6]

Fabrication of mesoporous TiO_2 particles has received more attention than their 1-D counterparts due to the difficulties associated with synthesizing these 1-D structures while still maintaining control of their dimensions. This is largely ascribed to the complexity associated with controlling the hydrolysis rate and the crystallization process of titanium precursor during particle growth. [7-11]

Attempts to synthesize 1-D structures with small dimensions and relatively large specific surface area have been made. [12-17] However, the synthesis of nanotubular or nanofibrous materials with good crystallinity could only be achieved by the templating method using porous anodic alumina. [7,10,18] The use of this method generates material with diameters larger than 50 nm as a result of the confinement of the molds used. The use of hydrothermal treatment of TiO_2, with either KOH or NaOH, proves to

be shorter and simpler and also yields high-quality tubes with uniform diameters (about 10 nm). Relatively large specific surface areas, in excess of 400 $m^2.g^{-1}$, can be obtained using a hydrothermal process. [14]

In this study we report on the effect of base concentration, temperature and base type on the formation of nanotubes which form bundles. New information about the mechanism of the formation of the tubes is provided.

II. Experimental Details

Materials. Titania (TiO_2 P25 Degussa, Germany), KOH (Merck, South Africa), NaOH (Merck, South Africa), lithium hydroxide (LiOH) (Merck, South Africa), ammonium hydroxide (NH_4OH) (Merck, South Africa) of analytical grades were all used without further purification. For all experiments deionised water was used.

Synthesis of TiO_2 Derived Nanostructures. The TiO_2-derived nanostructures in this study were all prepared using a standard hydrothermal procedure with conventional heating. The procedure is similar to that described by Kasuga and others elsewhere.[16, 19] In a typical synthesis method, 23 g of TiO_2 (P25 Degussa) was mixed with 200 ml of various concentrations (6, 10 or 18 M) of either LiOH, or NaOH or KOH. In certain experiments a NH_4OH (32 %) solution was used in lieu of alkali metal hydroxides. The mixture was then placed in a Teflon-underlined steel reactor and maintained at various temperatures (120 and 150°C) for 24 h. The reaction product of each experiment was then washed with deionised water. The solid was separated from the mixture by means of centrifugation at 4500 rpm for 15 minutes. Washing was repeated until a pH value of the supernatant of about 7-8 was attained. The product was then vacuum-dried in an oven at 120°C for 12 h and subsequently calcined at 300°C for 4 hours.

Characterisation. Nitrogen adsorption-desorption isotherms were measured on a Micromeritics TRISTAR 3000 analyser. Prior to analysis, samples were out-gassed at 150 ^{o}C in a vacuum for a few hours. The specific surface area of the nanostructures was determined by Brunauer-Emmett-Teller (BET) method.

The XRD analysis of the samples was carried out using a Phillips PW1830 diffractometer. The apparatus utilizes nickel-filtered CuK-α radiation (1.54 Å). The diffraction patterns were collected with an X-ray gun, operated at 40 kV and 20 mA.

Information on the morphological features of the samples was collected using transmission electron microscopy (TEM, on a JEOL 100S microscope). TEM samples were prepared by dispersing the powder in alcohol, followed by ultrasonic treatment. A drop of the mixture was then placed on a copper grid, coated with carbon support film.

Further morphological analysis was carried out using scanning electron microscopy (SEM). SEM measurements were made on a JEOL JSM-840 scanning electron microscope. Prior to analysis the samples were sputter-coated with a thin layer of gold.

The Raman analysis was carried out on a Jobin-Yvon T64000 spectroscopy, equipped with an Olympus BX-40 microscope attachment. The excitation wavelength of 514.5 nm, with an energy setting of 1.2 mW from a Coherent Innova Model 308 Argon ion laser, was used.

III. Results and Discussion

TiO_2 derived nanostructures were obtained by hydrothermally treating TiO_2 (P25 Degussa) with alkali metal hydroxides (LiOH, NaOH and KOH) and ammonium hydroxide (NH_4OH). The effects of base strength and the nature of reactivity with TiO_2 were investigated and the results are discussed.

Syntheses of titanate materials with tubular structures, using bases such as NaOH, KOH and LiOH have previously been attempted and reported. [6,17] Factors such as temperature, base concentration and

type have been reported to influence the formation of tubular structures. [20] It is generally acceptable, in the literature that variation of KOH concentrations leads to the formation of nanobelts or nanorods. [21] Most synthesis procedures utilized involve the use of acid treatment step to remove excess base. We report on the alkaline comparative study carried out in the absence of acid treatment step. We have found that the use of both NaOH and KOH generate nanotubular structures. Interestingly, KOH treatment also leads to the formation of new structures.

Textural Characterization of the samples. All materials synthesized in this study are listed in **Table 1** which shows the BET surface areas and the pore volumes of the materials used. Materials treated with KOH (**Samples A1**-**A4**), NaOH (**Samples B1**-**B4**) and LiOH (**Samples C1**-**C2**) showed larger surface areas than that of the starting material, TiO_2 (49 m^2/g). The largest surface area of 263 m^2/g was obtained for material treated with 18 M of KOH at 150 ^oC. Although treatment of TiO_2 with NH_4OH resulted in a slight decrease in surface area (**Samples D1**-**D2**), it is evident that materials treated with both LiOH and NH_4OH did not vary much. The samples were also comparable to TiO_2 in terms of the surface area and porosity. Both the surface area and pore volumes of the materials seem to have increased in accordance with the base strength, i.e. KOH>NaOH>LiOH>NH_4OH. This shows that the surface enlargement phenomenon is influenced by the nature and strength of the base. It is evident that treatment with relatively stronger bases (i.e. KOH and NaOH) results in the formation of more porous material. Moreover, treatment with relatively weaker bases (i.e. LiOH and NH_4OH) did not alter the surface area of TiO_2.

Microscopy Analysis. Figure 1 shows the morphological properties of TiO_2 (P25-Degussa) material used as a starting material in this study. The material consisted of clusters or agglomerates of particles that are somewhat spherical.

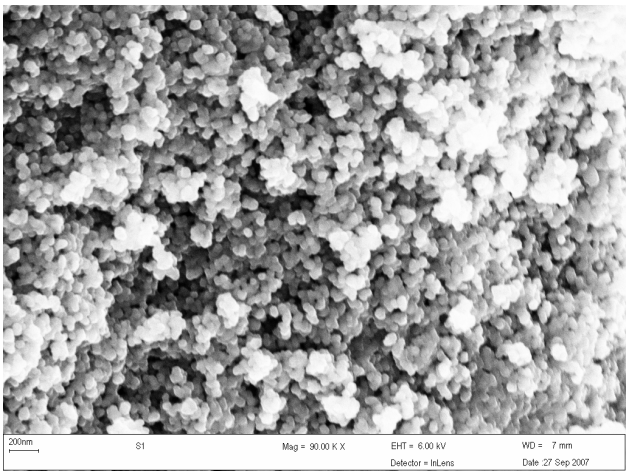

Figure 1. SEM image of untreated TiO_2 (P25-Degussa)

However, the spherical morphology of the starting material transformed into nanotubular morphology after treatments with 10 M of KOH at 120°C for 24 hours (**Sample A1**) and 10 M of KOH at 150 ^{o}C for 24 hours (**Sample A2**) as shown in **Figure 2**.

Sample A1 showed the presence of tubes with a small proportion of undeveloped or amorphous material. The tubes were randomly distributed and had a diameter range of 8-11 nm and lengths of a few hundred nanometers. The tubes were open-ended on both sides and had thin walls. Some of these tubes formed bundles. The amorphous material formed clusters of particles while some of these particles were deposited on the surface of the tubes (**Figure 2a**).

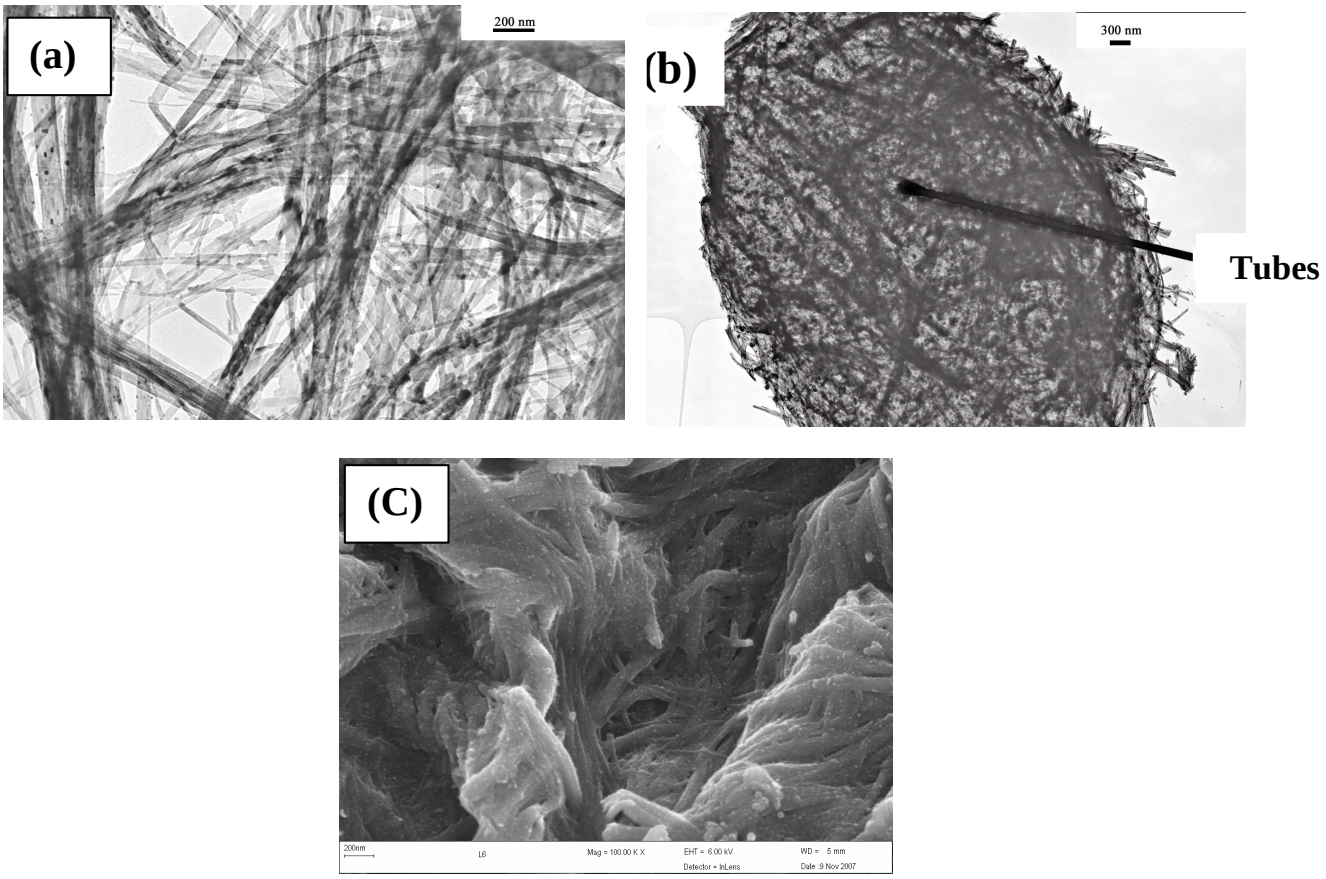

Figure 2. TEM images of (a) **Sample A1** treated with 10 M of KOH at 120 ^{o}C (b) **Sample A2** treated with 10 M of KOH at 150 ^{o}C; and (c) SEM image of **Sample A2** showing tubes covered with sheets.

Sample A2 did not show the presence of undeveloped material. The material was largely composed of tubes and a few unrolled sheets. However, some of the tubes randomly stuck together to form a ball-like structure (**Figure 2b**). The SEM image of **Sample A2** in **Figure 2c** shows the presence of what looks like tubes in a polymer matrix. It is believed that tubes that formed a ball-like structure are covered by film or sheet. It is well known that sheet formation is an intermediate step in hydrothermal synthesis of TiO_2 based nanotubes in the presence of a base such as NaOH. [22,23] The synthesis

conditions used might not be conducible for a complete roll-up of all sheets to form tubes. The ball-like structure was formed by the agglomeration of tubes and sheets.

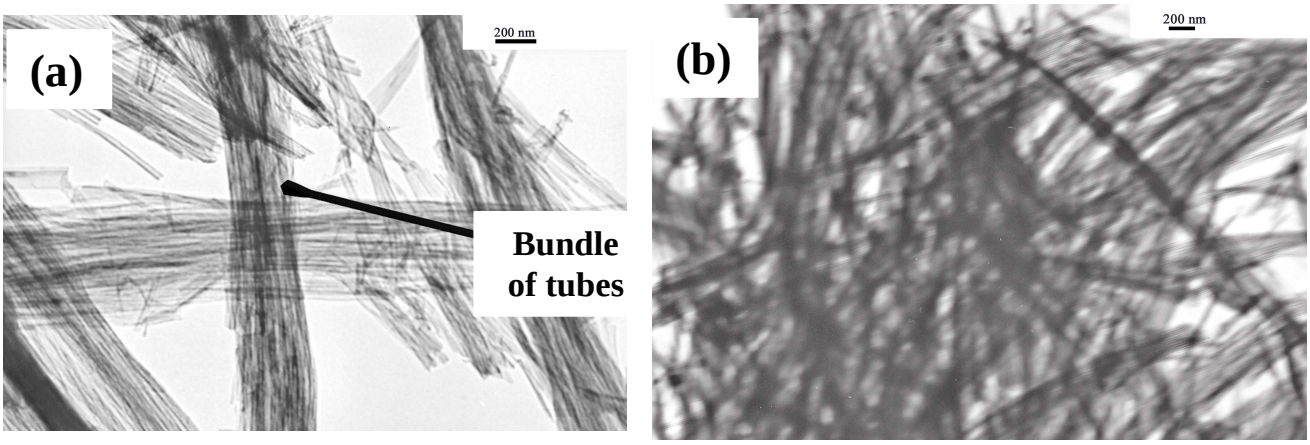

Figure 3. TEM images of TiO_2 treated with (a) 5 M KOH (**Sample A3**) and (b) 18 M KOH (**Sample A4**) at 150 ^{o}C.

The TEM micrograph of **Sample A3** (treated with 5 M of KOH at 150 ^{o}C) is shown in **Figure 3a**. **Sample A3** showed the presence of tubes, rods and amorphous material. The tubes formed bundles. Furthermore, when the concentration of KOH was increased to 18 M at 150°C (**Sample A4**) an increase in the yield of tubes to 100% resulted. The tubes were uniform with a narrow size distribution and had an average diameter of 10 nm. The tubes are relatively longer than those obtained at lower concentrations. The tubes were open-ended on either side and had thin walls. The TEM image of **Sample A4** shows that the tubes were randomly distributed and there was almost no aggregation (**Figure 3b)**. It is noteworthy that the highest yield of tubes that are somewhat perfect was attained when a solution of 18M of KOH was used. It is also interesting to note the largest surface area, 263 m^2/g, was obtained when 18 M of KOH was used whereas the lowest surface area was obtained when 5 M of KOH solution was used. The large surface area in **Sample A4** is attributed to the tubular structures whereas the low surface area in **Sample A3** is due to a relatively larger amount of amorphous material. The surface area of **Sample A3** (117 m^2/g) is larger than that of the starting

material (49 m^2/g) and is due to the presence of tubular structures. The concentration of KOH solution influenced the quality, yield and length of tubes, but not the tube diameter. The temperature also influenced the yield of tubular structures.

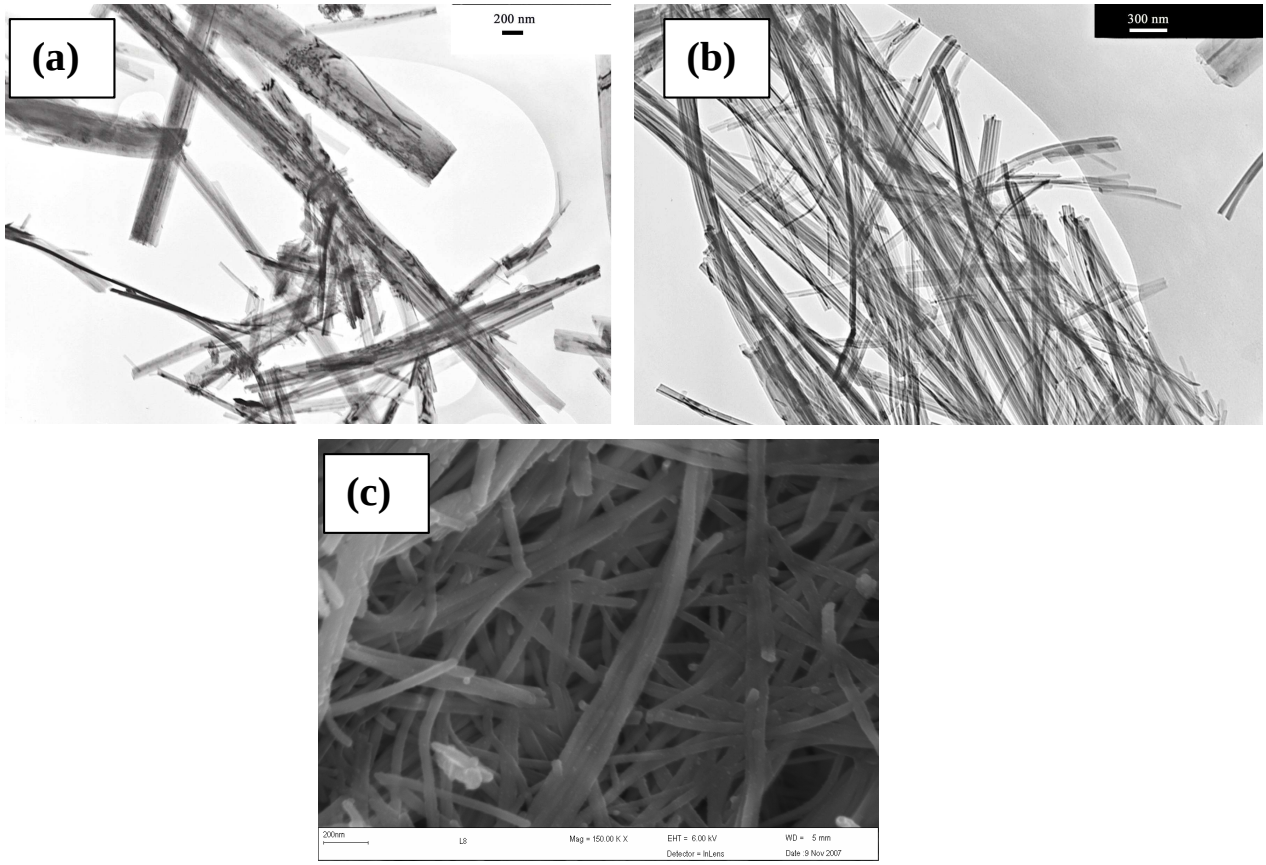

Figure 4. TEM images of TiO_2 (P25-Degussa) treated with (a) 10 M of NaOH at 120 ^oC for 24 hours (**Sample B1**) and (b) 10 M of NaOH at 150 ^oC for 24 hours (**Sample B2**); and (c) SEM image of **Sample B2**.

The TEM image of **Sample B1** (10 M NaOH at 120°C) in **Figure 4a** shows that the sample consisted of tubular and rod-like structures. The rod-like structures showed a wider diameter distribution than tubular structures. A significant amount of undeveloped material was also observed. The tubes formed

bundles and tended to break in the middle, resulting in length reduction. The tubes had an average diameter of 10 nm. Raising the temperature to 150°C (**Sample B2**) resulted in the formation of tubular structures with a 100 % yield (**Figure 4b**). The tubes were relatively longer than those in **Sample B1** and had an average diameter of 10 nm. Although most tubes were free from agglomeration, slight formation of bundles was observed with TEM analysis. Though SEM sample preparation does not include dispersion procedures such as ultrasonic dispersion technique the SEM image of **Sample B1** (**Fig. 4c**) shows the presence of bundles similar to those observed with TEM. This shows that ultrasonic procedure could not separate the bundled up tubes. However, tubes were randomly orientated.

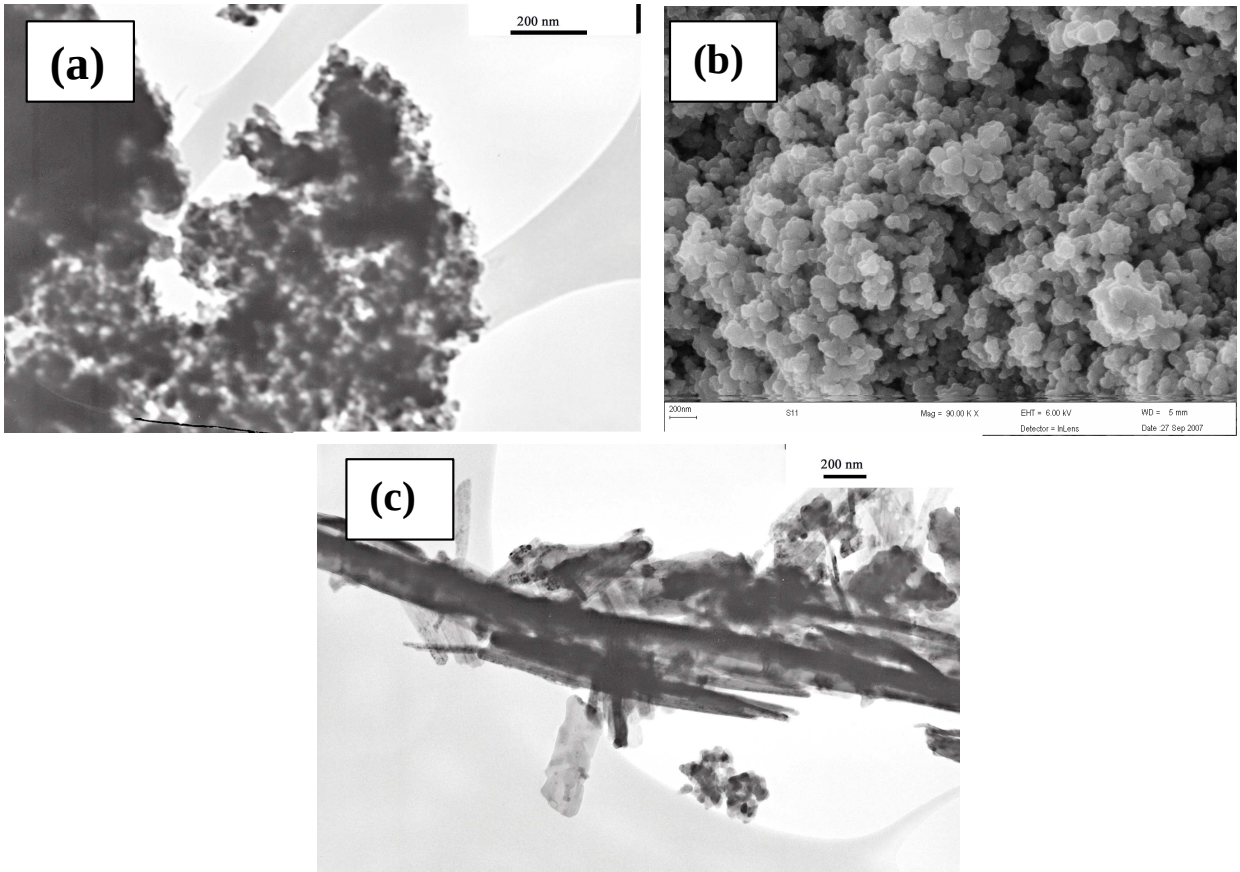

Figure 5. TEM image of TiO_2 treated with (a) 5 M NaOH (**Sample B3**), (b) SEM image of **Sample B3** and (c) 18 M NaOH (**Sample B4**) at 150°C.

On the other hand, when the concentration of NaOH was decreased to 5M under the same experimental condition **(Sample B3)**, there was no formation of tubular structure (see parts a and b of **Figure 5**). The sample consisted of clusters of particles similar to those of the starting material. However, when the concentration of NaOH solution was increased to 18 M from 10M under the same experimental conditions (**Sample B4**), a very small proportion of starting material was converted to tubes (~1 %, **Figure 5c**). Although the quantity of tubes was very small, the tubes were fully developed with diameters comparable to that of **Sample B2,** but shorter. However, the largest surface area, 247m^2/g, was obtained when 10 M of NaOH was used.

It was observed that the surface area increased with an increase in concentration of NaOH. However, the surface area of **Sample B4** (93 m^2/g) was smaller than that of **Sample B3** (107 m^2/g). The lower surface area observed for **Sample B4** is probably due to the formation of tubular structures which subsequently re-dissolved to form amorphous material. This might lead to the formation of larger crystals than those of **Sample B3.** The concentration of NaOH largely influenced the formation and length of tubular structures.

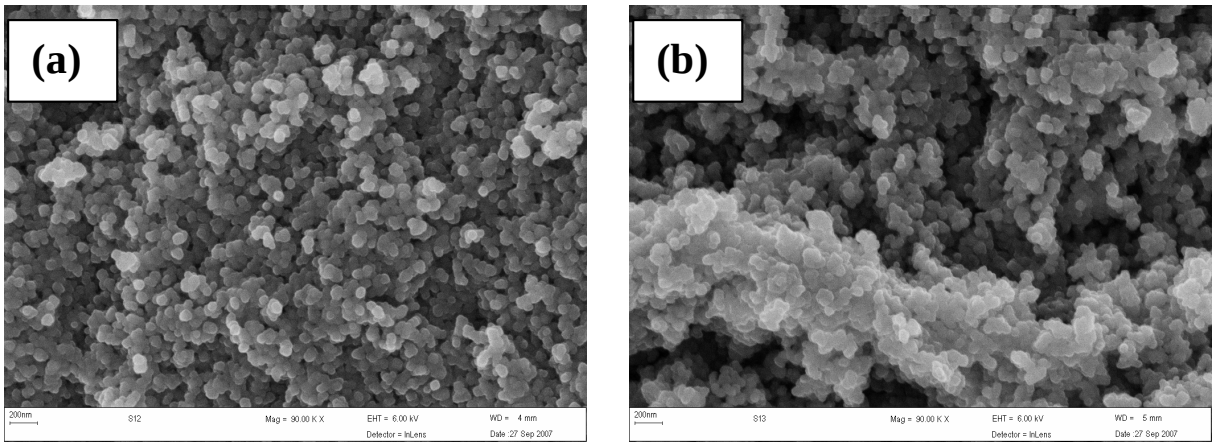

Figure 6. SEM images of TiO_2 treated with (a) 10 M of LiOH at 120°C (**Sample C1**) and (b) 10 M of LiOH at 150°C (**Sample C2)**.

The SEM images of **Samples C1** and **C2** are shown in **Figure 6(a)** and **(b)**, respectively. The images depict similar microstructures for both samples. The microstructures displayed by these samples (**Samples C1** and **C2**) are similar to that of the starting material (TiO_2, P25-Degussa) shown in **Figure 1**. All three samples showed comparable particle shape and size with a regular spherical morphology. It is noteworthy that although **Samples C1** and **C2** had similar morphology they had different surface areas (51 and 60 m^2/g respectively). The surface area of **Sample C1** and that of the starting material were rather comparable suggesting that treatment of TiO_2 with LiOH at 120°C, does not alter the microstructure and the surface properties of the TiO_2. However, a slight improvement in surface area was observed when the temperature was elevated to 150°C. The similar particulate morphology suggests that the larger surface area in **Sample C2** is probably due to intra- and inter-particle porosity. This is consistent with the observed larger pore volume.

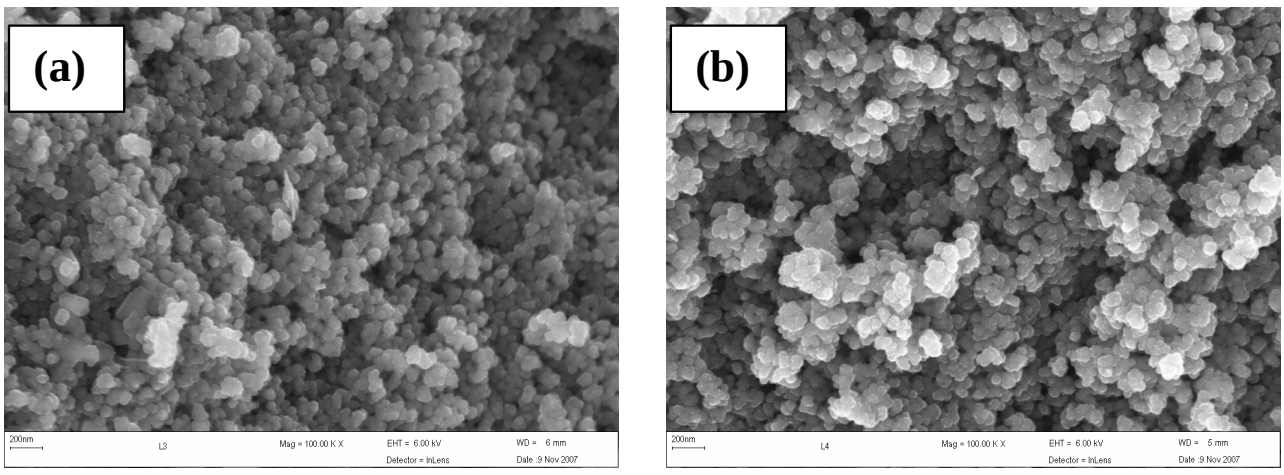

Figure 7. SEM images of TiO_2 treated with (a) 32% of NH_4OH at 120 ^oC (**Sample D1**) and (b) 32% of NH_4OH at 150°C (**Sample D2**).

The SEM images of samples treated with 32% NH_4OH at 120 and 150°C (**Samples D1** and **D2**) are shown in **Figs. 7(a)** and **(b)** respectively. The microstructures of both materials were similar to each other and to that of TiO_2. The surface areas were also comparable to that of TiO_2. This clearly shows that NH_4OH has no influence on the microstructure of TiO_2. The observed slight decrease in surface area with increasing temperature is ascribed to grain growth.

XRD Analysis. The XRD patterns of **Samples A1**-**A4** are shown in **Figure 8**. The XRD patterns of **Samples A1** and **A3** (shown in inset) showed a few peaks at 2-theta values of 25 and 27°, which are characteristic of the anatase and rutile phases of TiO_2, respectively. This indicates samples are relatively more crystalline. The TiO_2 peaks are attributed to the presence of unreacted material in both samples. The pattern also shows the broadening of other peaks due to the presence of nanotubular structures. **Samples A2** and **A4** show more peaks broadening than those of **Samples A1 and A3**. This is due to the presence of larger quantities of tubular structures in the corresponding samples. The assignment of these few peaks to any of the known crystal structures is not possible; however, the peak broadening is indicative of the presence of nanocrystals.

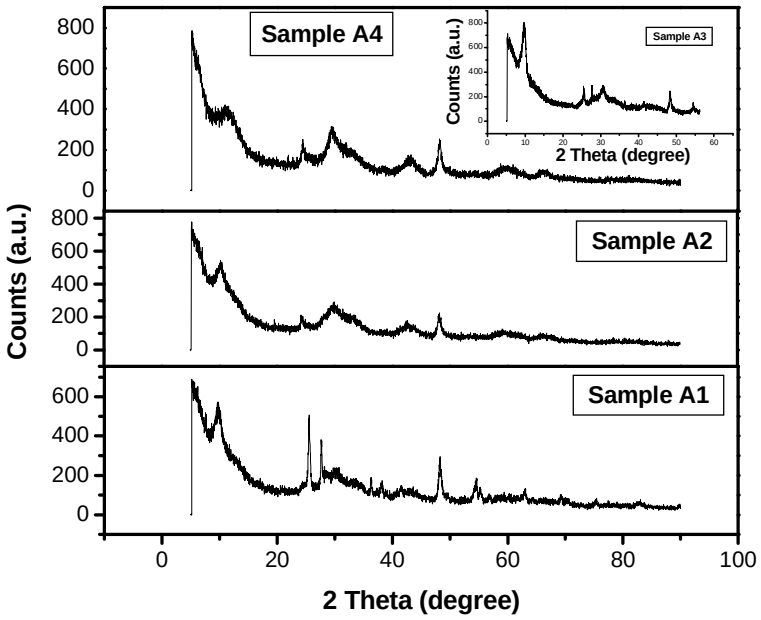

Figure 8. XRD patterns of **Samples A1**-**A4**.

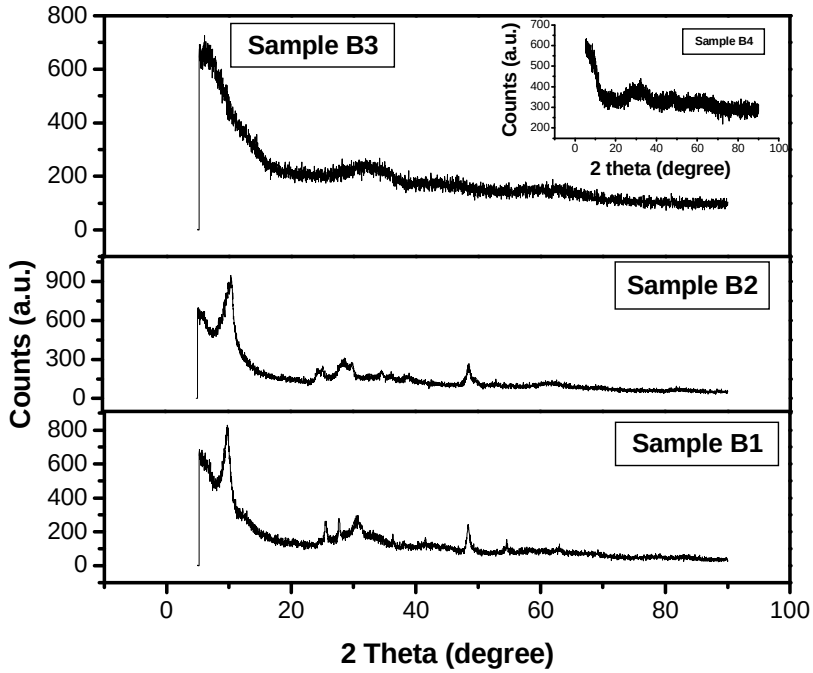

Figure 9. XRD patterns of **Samples B1**-**B4.**

The XRD patterns of **Samples B1**-**B4** are shown in **Figure 9**. The XRD pattern of **Sample B1** shows the presence of a few characteristic peaks of TiO_2 which are due to the presence of the un-reacted material. **Sample B2**, which is more crystalline than **Samples B3** and **B4**, shows peak broadening due to the presence of nano-sized tubular structures. The peaks broadening in **Samples B3** and **B4** suggest that at an elevated temperature (150 ^{o}C) and a NaOH concentration less/greater than 10 M TiO_2 particles are transformed into smaller particles. TiO_2 particles might form tubes, during synthesis, which subsequently re-dissolved to form smaller crystals rendering tubular structures unstable at concentrations of NaOH lower and/or higher than 10 M.

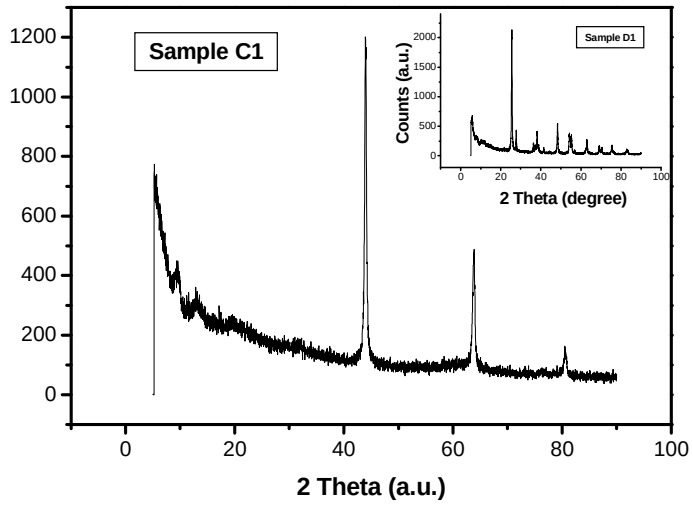

Figure 10. XRD patterns of **Sample C1** and **Sample D1**.

The XRD patterns of **Sample C1** (**Figure 10**) and **Sample C2** (not shown) were found to be identical. It is interesting to note that the XRD pattern of **Sample C1** revealed the presence of very few and new crystalline peaks at 2-theta values of ~44, 64 and 81°, which could not be indexed to either the anatase or rutile phase. The peaks were found to correspond to that of $LiTiO_2$ phase using the Expert High

Score 2002 software and XRAYAN software developed at Unipress, Institute of High Pressure Physics in Poland. It was found that with an increase in the LiOH concentration, the $LiTiO_2$ phase became more prominent with increasing peak intensity.

The XRD patterns of **Sample D1** (**Figure 10**, inset) and **Sample D2** (not shown) were found to be identical. This clearly shows that treatment of TiO_2 with NH_4OH has no influence on the crystal structure. Though treatment with NH_4OH resulted in an increase in system pressure due to the formation of ammonia, however, this did not influence the reactivity with TiO_2.

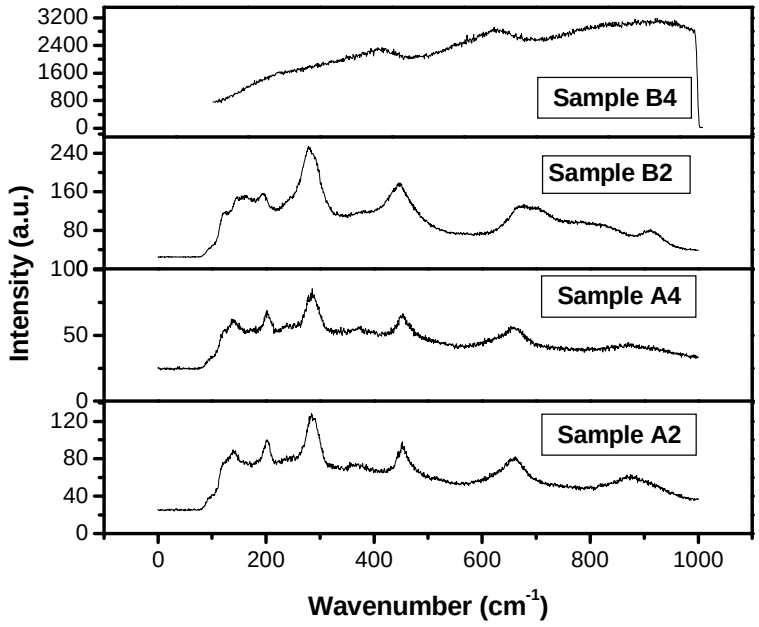

Figure 11. Raman spectra of **Samples A2**, **A4**, **B2**, and **B4**.

Raman Spectroscopy. The Raman spectra of **Samples A2**, **A4**, **B2** and **B4** are shown in **Figure 11**. All samples showed the presence of new peaks that are neither of anatase nor rutile phase. These peaks are primarily due to the structural changes in the TiO_2, resulting from the transformation of 3-D crystallites to 1-D nanotubes. The peaks observed at 188, 271, 441, and 652 cm^{-1} for **Samples A2**, **A4**,

and **B2** are all attributed to a titanate structure. [24,25] **Sample B4** showed peaks much broader than other samples due to small particle-size, implying the absence of ordered crystallinity. This observation is consistent with the XRD results. The broader peaks observed at 271, 441, 652 and 905 cm^{-1} for **Sample B4** are also attributed to a titanate structure. The peaks at 271 and 441 cm^{-1} are assigned to the Ti-O-M (M = Na^+ or K^+) bonding in the titanate structure. [26] This clearly suggests that the nanotubes and NaOH-treated particles are made from a titanate structure containing either K or Na. Energy dispersive X-ray (EDX) spectroscopy studies showed that all samples contained Ti, O and M (where M = Li, Na or K). This finding is consistent with titanate structures with the formulae of $Na_2Ti_2O_4(OH)_2$ and $KTiO_2(OH)$. [27,28]

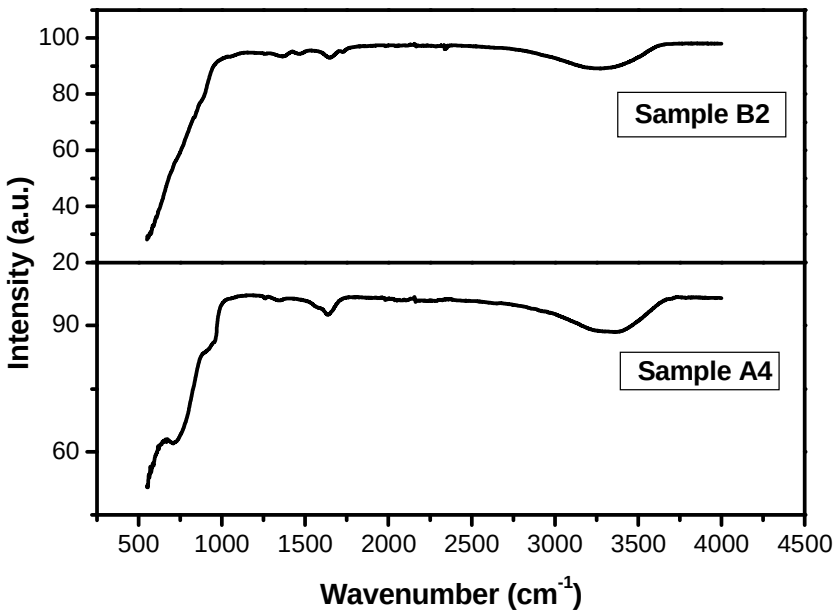

Figure 12. FTIR spectra of **Samples A4** and **B2** recorded at room temperature.

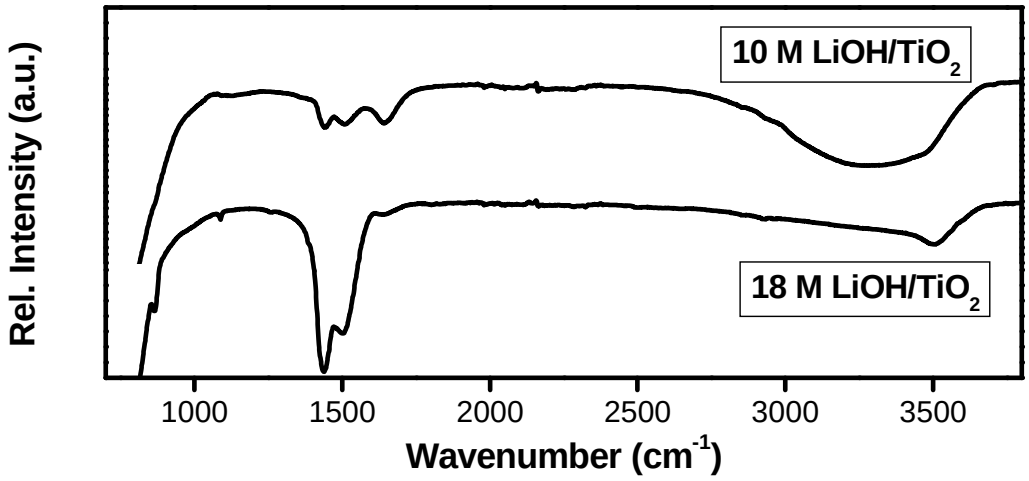

Figure 13. FTIR spectra of **Samples A4** and **B2** recorded at room temperature.

FTIR spectroscopy. A FTIR spectroscopy was used to show the presence of '-OH' group in the titanate structure and shown in **Figure 12**. The two OH stretch vibrations observed at 3600-2600 and 1625 cm^{-1} for both **Sample A4** and **Sample B2** are due to two different chemical environments of the OH groups.[29] The OH bands at ~3600 cm^{-1} did not disappear, even when the samples were heated at high temperatures (~200°C). [27] This clearly shows that the absorption bands could be considered to be the part of the crystal lattice and consistent with the Raman spectroscopy results as discussed previously.

Figure 13 shows the FTIR spectra of nanocrystalline $LiTiO_2$. Both spectra show peaks characteristic of the OH group at 3430 and 1636 cm^{-1}. [30] The broader peaks centred at 3430 cm^{-1} are OH stretching vibrations of surface hydroxyl groups. [30] The absorption peaks at 1636 cm^{-1} are due to physically adsorbed water molecules (H-O-H). [31] Two more peaks were observed at 1505 and 1435 cm^{-1} and their relative intensity increase with an increase in LiOH concentration. The two peaks are attributed

to the stretching vibration of Li-O-Li bonding. [32] The increase in peak intensity with LiOH concentration is due to the increase in the amount of $LiTiO_2$ phase.

Table 1: BET surface areas and pore volumes. All samples were hydrothermally treated for 24 hours.

Designation	**Precursor**	**Temperature (^oC)**	**Base Concentration (mol/L)**	**S_{BET} (m^2/g)**	**Pore Volume (cm^3/g)**
TiO2	P25 Degusaa	-	-	49.4	0.33
Sample A1	KOH/TiO_2	120	10	154	0.44
Sample A2	KOH/TiO_2	150	10	204	0.62
Sample A3	KOH/TiO_2	150	5	117	0.38
Sample A4	KOH/TiO_2	150	18	263	0.84
Sample B1	$NaOH/TiO_2$	120	10	143	0.46
Sample B2	$NaOH/TiO_2$	150	10	247	0.75
Sample B3	$NaOH/TiO_2$	150	5	107	0.49
Sample B4	$NaOH/TiO_2$	150	18	93.4	0.39
Sample C1	$LiOH/TiO_2$	120	10	51.0	0.37
Sample C2	$LiOH/TiO_2$	150	10	59.8	0.43
Sample D1	NH_4OH/TiO_2	120	32 %	47.7	0.41
Sample D2	NH_4OH/TiO_2	150	32 %	43.9	0.38

Comparison. From the above results it is clear that the main products in this study are **Samples A2, A4** and **B2**. A detailed study of the effect of variation of base concentration on tubular structures at low temperature (120°C), has been reported elsewhere. [20]

The textural data for the samples are summarized in **Table 1**. The BET specific surface areas of the samples containing only tubular structures (viz. **Sample A4** and **Sample B2**) were 5 times higher than that of commercial material. The surface area increased with an increase in the quantity of tubular structures and was independent of the base used. The increased specific surface area for the tubular

materials is influenced by the porous nature of the tubes. The increased surface areas of the non-tubular materials are probably due to increased intra- and inter-particle porosity. The increase in surface areas of LiOH-treated samples (**Samples C1-C2**) is probably due to the insertion of Li^+ into the structural framework of TiO_2 resulting in an increased porosity.

The yield of the tubes increased with an increase in temperature (from 120°C to 150°C) for both NaOH- and KOH-treated samples. This shows that the tube formation can be kinetically controlled. However, LiOH- and NH_4OH-treated samples did not show any dependence on the temperature range. The concentration of the base was found to influence both the yield and morphology of the materials. The formation of rod-like structures in **Samples A3** and **B1** might have resulted from the agglomeration of the tube bundles. The highest yield of tubes (~100 %) was obtained when the concentration of KOH was 18 M at 150°C. At concentrations lower than 18 M (*i.e.* 5 and 10 M) of KOH under the same experimental condition, tubes and/or rod-like structures with imperfections were obtained. Tubes appeared shorter with a wide particle length distribution. It appeared as though longer tubes were initially formed and then broke into shorter pieces with different sizes. The tube fracture is believed to be due to tube instability in base concentration. This clearly shows that depending on the experimental conditions new defects may be introduced into the tubular structures. Bundle-formation was observed. However, a different kind of behavior was noticed with NaOH treated samples. The highest yield (~100 %) of tubes was attained when the concentration was 10 M at 150°C. At concentrations lower or higher than 10 M, very little or no tubes were formed. Yuan and co-workers had similar observations for NaOH-treated samples. [20] Our data clearly show that the variation of concentration and temperature not only affects the morphology and particle-size but also the orientation of the nanostructures (i.e. formation of bundles, rods and spherical structures). The bundle formation is taking place by the self-assembly of tubular structures. This could be due to charge accumulation on the surface of tubes thereby increasing an electrostatic attraction between the tubes.

Based on the morphological data it can be inferred that the formation of bundle-like structures is largely affected by the concentration and the nature of a base. It is interesting to note that all the tubular structures formed (i.e. NaOH and KOH) showed similar diameter suggesting that crystal growth mechanism was not sensitive to type of base used. However, the threshold concentration for the formation of nanotubes is higher for KOH than NaOH. The formation of other structures such as nanorods, sheets and ball-like structures were obtained below the threshold concentration for tube formation with KOH. To the best of our knowledge the formation of a ball-like structure of TiO_2 derived nanotubes has not been reported before. The presence of sheets and tubular structures at a specific base concentration and temperature is believed to be responsible for the interconnectivity of tubes to form a ball-like structure. The tubular and sheet-like structures might have aggregated through physical attraction due to surface charges. The dangling bonds of the two-dimensional lamellar (sheet) could also interact with the surface atoms of the free and bundled tubular structures via weak van der Waals forces leading to the formation of larger and complicated ball-like structure. This effect might have kinetic reasons. It appears that the rolling up process of the 2-D structures (sheets) is slower than the formation process thereby increasing possible interaction of the already formed tubes with these structures (sheets). This is probably due to insufficient concentration of KOH (i.e. 10 M) required for rapid formation of tubes.

Variation in the concentration of NH_4OH showed no influence. A new phase ($LiTiO_2$) was observed with LiOH and the XRD peaks increased with an increase in the concentration of LiOH. The data show that the tube formation was dependent on the reactivity and strength of the base. Of the four bases, KOH is the strongest and readily transformed the morphology of the starting material. Although LiOH is a strong base (weaker than NaOH and KOH) no tubular structures or morphological changes were observed. This is possibly due to a relatively smaller size of Li^+ which

might not be compatible with the lattice of TiO_2. The difference in optimum concentrations for tube yield for both KOH and NaOH is attributed to thermodynamic stability.

Previous studies have suggested that treatment of TiO_2 with KOH leads to the formation of only rod-like structures. [20] We have found that the bundles of tubes may coexist along with rod-like structures depending on conditions used but when the base concentration was high (i.e. 18 M) tubes free from agglomeration could be produced. Early studies have suggested that the tube formation is underpinned by the acid treatment step. [26,33] However, recent studies have shown that the acid treatment step is not crucial for the formation of tubes. [17,19] Our results suggest that the acid treatment step is not required and that tubular structures can only be formed when the correct base, base concentration and temperature are utilized. Though the Li^+, Na^+ and K^+ ions could penetrate the lattice of TiO_2 it is known that these ions could be replaced by H^+ to form a proton titanate with or without a tubular structure. This shows that tubular structures obtained by acid treatment might have a different structure and properties when compared with those not treated. Acids used to convert the alkali metal ion titanates to H-form titanate include HCl and HNO_3 among others. [14] This further contaminates the products and introduces defects. [13,17] The removal of chloride ions is especially difficult. It is known that acid treatment reduces the dimensions (length shortening) of both single-walled and multi-walled carbon nanotubes (SWCNT and MWCNT) and introduces new defects. [34-36]

Both NaOH and KOH-treated tubular samples showed broadening of diffraction peaks mainly due to the nanometer-size of the tubes and the bending of some atom planes of the tubes.

It was observed that samples treated with KOH became fluffy with increased volume and decreased density. This is attributed to lattice expansion of the TiO_2 matrix due to the intercalation of K^+ ions which have larger ionic radii than Ti^{+4} ions. This effect was not observed for NaOH-treated samples and it is believed that this is because of the ionic radius of Na^+, though numerically larger, is comparable to that of Ti^{+4}. The ionic radius of Li^+ is relatively smaller than that of Ti^{+4}. High levels of

basicity and concentration of alkali metal ions favor the formation of titanate phases, i.e. $LiTiO_2$, $KTiO_2(OH)$ and $Na_2Ti_2O_4(OH)_2$. It can be concluded that treatment of TiO_2 with alkali hydroxides (LiOH, NaOH and KOH) leads to the formation of titanate structures with respective alkali metal ions intercalated. The formation of denser $LiTiO_2$ nanocrystals with smaller dimensions than those of the starting materials (TiO_2) suggests that Li^+ could occupy the position of Ti^{+4} via substitution. The intercalation of Li^+ appears to have a phase stabilizing effect probably due to its relatively smaller ionic size than that of Ti^{+4}. The intercalation of Na^+ and K^+ destabilize the TiO_2 framework forming a sheet and subsequently tubular structures (or rods). However, the formation of tubular structures is underpinned by the size of the metal ions. Furthermore, the nature and concentration of the base used also influences the morphology (i.e. the formation of spherical or rod-like particles). Previous studies have suggested that treatment of TiO_2 with KOH leads to the formation of nanowires. [20] We have shown that by using very concentrated solution of KOH (i.e. 18M) tubular structures that are somewhat perfect could be formed. However, variation of KOH concentration yielded different structures such as nanorods.

Nanotubes Formation Mechanism. Tubular and non-tubular structures were obtained after treatment with various concentrations of NaOH and KOH solutions. The powder XRD and Raman data revealed that structural changes occurred despite the final particle morphology. The structural changes were accompanied by improved BET specific surface areas. Samples without tubular structures such as **Samples B3** and **B4,** showed an increase in the specific surface area. Samples prepared from KOH were fluffy and bulky.

Based on our results, the mechanism of formation of tubes is proposed to occur as shown in **Scheme 1**. When crystalline particles of TiO_2 material are treated with a very concentrated LiOH or NaOH or KOH solution the metal ions (Li^+ or Na^+ or K^+) are intercalated into the TiO_2 framework. When both

the temperature and base concentration are sufficiently high enough, intercalation of ions occurs. This is followed by the exfoliation of three-dimensional crystallites into two-dimensional layered sheets. The exfoliation is due to destabilization of TiO_2 structure by metal ions (i.e. Na^+ or K^+). However, Li^+ forms a stable phase (i.e. Li^+ too small to destabilize TiO_2 lattice). The edges of the layered structures might contain atoms with dangling bonds. The layered sheets are unstable mainly because of high system energy (high surface-to-volume ratio). In order to reduce the system energy by saturating surface dangling bonds the two-dimensional structures roll up, thereby forming one-dimensional tubes.[22, 23] This shows that the intercalation of ions and the formation of the intermediate product (two-dimensional sheets) are crucial steps in the formation of tubes.

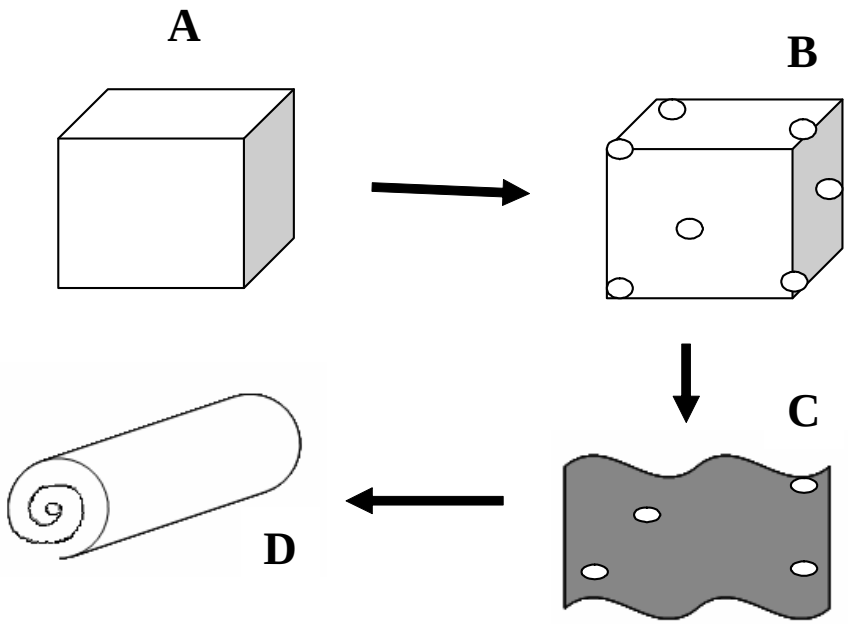

Scheme 1. Mechanism of nanotubes formation.

IV. Conclusions

In the present study, the effect of base concentration, temperature and the type of base on the formation of nanotubes have been investigated systematically. On the basis of results and discussion the following conclusions can be made: First, the nanotubular structures can be produced hydrothermally by treatment of TiO_2 with either NaOH or KOH, under controlled conditions. Second, KOH is more reactive with TiO_2 to yield nano-structured materials with different shapes than does NaOH. Nanotubular structures were successfully synthesized in the absence of an acid treatment step using KOH and leading to the formation of a more complicated ball-like structure. The shape and nature of nano-structured material formed are influenced by the concentration of KOH used, and the yield of nanostructures is influenced by both temperature and base concentration. Fourth, the formation of tubes is preceded by metal ion intercalation, followed by the formation of a two-dimensional layered structures and subsequently tubes. Fifth, the basicity and the metal ion compatibility for intercalation are crucial for the formation of tubes. Although LiOH is also a strong base, it is relatively weaker than both NaOH and KOH. Li^+ ion has a smaller ionic radius than Na^+ and K^+. Finally, although the pressure in the reactor system may be important for the formation of tubes, it is clear that the basicity overrides the effect of pressure. The use of NH_4OH increased the system pressure due to the formation of NH_3. No chemical transformation of TiO_2 was observed. This is partly due to the lack of metal ion to be intercalated and the weakness of NH_4OH as a base.

Acknowledgements. LMS and SSR thank the CSIR executive and DST, SA for financial support.

References and Notes

[1] J.G. Yu, H.G. Yu, B. Cheng, X.J. Zhao, J.C. Yu, W.K. Ho, J. Phys. Chem. B 107, 13871 (2003)

[2] F.B. Li, X.Z. Li, M.F. Hou, Appl. Catal. B: env. 48, 185 (2004)

[3] J.G. Yu, X.J. Zhao, Q.N. Zhao, J. Mater. Res. 7, 379 (2000)

[4] J.C. Zhao, T.X. Wu, K.Q. Wu, K. Oikawa, H. Hidaka, N. Serpone, Environ. Sci. Technol. 32, 2394 (1998)

[5] M. Adachi, Y. Murata, M. Harada, S. Yoshikawa, Chem. Lett. 8, 942 (2000)

[6] H. Peng, G. Li, Z. Zhang, Mater. Lett. 59, 1142 (2005)

[7] P. Hoyer, Langmuir 12, 1411 (1996)

[8] B.B. Lakshmi, P.K. Dorhout, C.R. Martin, Chem. Mater. 9, 857 (1997)

[9] S.M. Liu, L.M. Gan, L.H. Liu, W.D. Zhang, H.C. Zeng, Chem. Mater. 14, 1391 (2002)

[10] S. Lee, C. Jeon, Y. Park, Chem. Mater. 16, 4292 (2004)

[11] M.S. Sander, M.J. Cote, W. Gu, B.M. Kile, C.P. Tripp, Adv. Mater. 16, 2052 (2004)

[12] Q. Zhang, L. Gao, J. Sun, S. Zheng, Chem. Lett. 31, 226 (2002)

[13] G.H. Du, Q. Chen, R.C. Che, Z.Y. Yuan, L.P. Peng, Appl. Phys. Lett. 79, 3702 (2001)

[14] X. Meng, D. Wang, J. Liu, S. Zhang, Materials Research Bulletin 39, 2163 (2004)

[15] R. Ma, Y. Bando, T.J. Sasaki, T. J. Phys. Chem. B **2004**, 108, 2115

[16] T. Kasuga, M. Hiramatsu, A. Hoson, T. Sekino, K. Niihara, Langmuir 14, 3160 (1998)

[17] Q. Chen, W.Z. Zhou, G.H. Du, L.M. Peng, Adv. Mater. 14, 1208 (2002)

[18] Y. Lei, L.D. Zhang, G.W. Meng, G.H. Li, X.Y. Zhang, C.H. Liang, W. Chen, S.X. Wang, Appl. Phys. Lett. 78, 1125 (2001)

[19] L.M Sikhwivhilu, N.J. Coville, D. Naresh, K.V.R. Chary, V. Vishwanathan, Appl. Catal. A: Gen. 52, 324 (2007)

[20] Z.Y. Yuan, B.L. Su, Colloids and Surfaces A: Physicochem. Eng. Aspects 241, 173 (2004)

[21] X. Sun, X. Chen, Y. Li, Inorg. Chem. 41, 4996 (2002)

[22] B.D. Yao, Y.F. Chan, X.Y. Zhang, W.F. Zhang, Z.Y. Zhang, Z.Y. Yang, N. Wang, Appl. Phys. Lett. 82, 281 (2003)

[23] Y.Q. Wang, G.Q. Hu, X.F. Duan, H.L. Sun, Q.K. Xue, Chem. Phys. Lett. 365, 427 (2002)

[24] X.Y. Liu, N.J. Coville, S. Afr. J. Chem. 58, 110 (2005)

[25] S. Uchida, R. Chiba, M. Tomiha, N. Masaki, M. Shirai, Stud. Surf. Sci. Catal. 146, 791 (2003)

[26] T. Kasuga, M. Hiramatsu, A. Hoson, T. Sekino, K. Niihara, Adv. Mater. 11, 1307 (1999)

[27] J. Yang, Z. Jin, X. Wang, W. Li, J. Zhang, S. Zhang, X. Guo, Z. Zhang, Dalton Trans. 3898 (2003)

[28] N. Masaki, S. Uchida, H. Yamana, T. Sato, Chem. Mater. 14, 419 (2002)

[29] X. Sun, Y. Li, Chem. Eur. J. 9, 2229 (2003)

[30] R. Wang, K. Hashimoto, A. Fujishima, M. Chikuni, E. A. Kojima, A. Kitamura, M. Shimohigoshi, and T. Watanabe, Adv. Mater., 10, 135 (1998)

[31] D. Dvoranova, V. Brezova, M. Mazura, and M. A. Malati, Appl. Catal. B: Environ., 37, 91 (2002)

[32] G.S. Gopalakrisna, S.P. Madhu, M. Mahendra, M.J. Maheshu, M.A. Sridhara, P. Shashidhara, J. Mater. Lett., 60, 613 (2006)

[33] S.H. Chein, Y.C. Liou, M.C. Kuo, Synthetic Metals 152, 333 (2005)

[34] J. Zhang, H. Zou, Q. Qing, Y. Yang, Q. Li, Z. Liu, X. Guo, Z. Du, J. Phys. Chem. B: 107, 3712 (2003)

[35] T.J. Aitchison, M. Ginic-Markovic, J.G. Matisons, G.P. Simon, P.M. Fredericks, J. Phys. Chem. C: 111, 2440 (2007)

[36] Y. Kim, D. Lee, Y. Oh, J. Choi, S. Baik, Synthetic Metals 156, 999 (2006)